NASA Technical Memorandum 100063

The Present Status and the Future of Missile Aerodynamics

Jack N. Nielsen

January 1988

National Aeronautics and
Space Administration

NASA Technical Memorandum 100063

The Present Status and the Future of Missile Aerodynamics

Jack N. Nielsen, Ames Research Center, Moffett Field, California

January 1988

NASA
National Aeronautics and
Space Administration

Ames Research Center
Moffett Field, California 94035

SUMMARY

This paper reviews some recent developments in the state of the art in missile aerodynamics. Among the subjects covered are (1) Tri-service/NASA data base, (2) wing-body interference, (3) nonlinear controls, (4) hypersonic transition, (5) vortex interference, (6) airbreathers, supersonic inlets, (7) store separation problems, (8) correlation of missile data, (9) CFD codes for complete configurations, (10) engineering prediction methods, and (11) future configurations. Throughout the paper, suggestions are made for future research and development to advance the state of the art of missile aerodynamics.

SYMBOLS

a	body radius at wing position
AR	aspect ratio
b	span, wing tip to wing tip
C_A	axial force coefficient
C_ℓ	rolling moment coefficient
C_{ℓ_β}	effective dihedral, negative for stability
C_m	pitching moment
C_{NF}	normal force coefficient of fin
C^*_{NF}	value of C_{NF} at $\bar{\alpha}_\ell$ and $\bar{M}_\ell$ for wing alone
C_n	yawing moment coefficient
C_{n_β}	directional stability, positive for stability
D	drag of missile configuration
K_B	$N_{B(W)}/N_W$, body lift interference parameter for $\delta_f = 0$
K_W	$N_{W(B)}/N_W$, wing lift interference parameter for $\delta_f = 0$

K_ϕ	constant used to express change in fin angle of attack caused by $\alpha\beta$ coupling
k_1	$b/(\ell \tan \alpha)$
k_2	$M_\infty \sin \alpha$, cross-flow Mach number
k_3	$(\tan \alpha)/AR$
k_W	lift interference parameter for control; $N_{W(B)}/N_W$ with $\alpha_B = 0$, $\alpha_W = \delta_f$
L/D	configuration lift-drag ratio
ℓ	length of missile configuration
M_∞	freestream Mach number
M_c, M_n	Mach number normal to body axis
M_ℓ	local Mach number at a point in a flow
$\bar{M}_\ell$	average Mach number across exposed span of fin
N	configuration normal force
$N_{B(W)}$	normal force on body caused by presence of wing
N_W	normal force on wing alone (wing alone = two fins joined at root chord)
$N_{W(B)}$	normal force of wing in the presence of body
q_∞	freestream dynamic pressure
q_ℓ	local dynamic pressure
$\bar{q}_\ell$	average value of q_ℓ across exposed span of fin
r	radial distance of point from body longitudinal angle
r, ϕ	polar coordinates in crossflow plane
s, s_m	distance from body longitudinal axis to tip of fin
y	lateral distance from body longitudinal axis in plane of fins

$(\bar{x}/c)_F$	distance of fin center of pressure from leading edge of root chord nondimensionalized by fin root chord
α	angle of attack of undeflected fin, $\alpha_c \cos \phi$
α_c	angle of attack of missile body
α_{eq}	eauivalent angle of attack, Eq. (5)
α_ℓ	local angle of attack at a point in flow
$\bar{\alpha}_\ell$	average angle of attack across exposed span of fin
δ_f	angular deflection of fin from zero position
$\delta_1, \delta_2, \delta_3, \delta_4$	deflection of fin 1, etc.
ϕ	roll angle of right fin from its horizontal position, positive clockwise
λ	taper ratio of fin, ratio of tip chord to root chord at wing-body juncture
β	sideslip angle, $\beta = \alpha_c \sin \phi$ or $\sin \beta = \sin \alpha_c \sin \phi$ for large α_c
θ_c	semi-apex angle of cone
Λ_{jj}	an interference factor slightly less than unity associated with deflection of fin j

1. INTRODUCTION

In the six years since the last AGARD meeting on missile aerodynamics in Trondheim, Norway in 1982, much has happened. The purposes of the present paper are to describe the recent developments in missile aerodynamics, and to suggest areas where future research could be fruitful.

The emphasis in the paper is on the U.S. experience in stability and control of tactical missiles. The aerodynamic problems are discussed in generic terms so that reference to particular missiles is not necessary.

The paper covers theory, experiment, and engineering prediction, but not radar cross-section. The papers of the 1982 AGARD meeting are to be found in reference 1.

2. OVERVIEW

Among the aerodynamic requirements for tactical missiles are range, maneuverability, and speed. These requirements can be contradictory depending on the specific application. The search for range has led to much work on airbreathing missiles. As a consequence, there is an interest in noncircular, nonrolling missiles. The desire for maneuverability has led to operation at high angles of attack, which, in turn, has created serious stability and control problems. At the same time, the use of airbreathers puts definite angle-of-attack limits under which the engines will operate, and in this regard, range and maneuverability are in conflict.

The trend toward higher speeds has brought with it new problems in hypersonic aerodynamics such as wing-body interference effects and unusual vortex behavior. In addition, there are the questions of transition and turbulence at hypersonic speeds which are important in many applications.

Methods of calculating the aerodynamics of missiles have been improved and recent developments have increased the accuracy of the Euler equations for calculating missile flow fields. An engineering method for the design of missiles has been produced in MISSILE DATACOM (ref. 31).

Also an engineering design code which works to high angles of attack, Missile III, has been developed based on an extensive Tri-service/NASA data base (ref. 2).

3. TRI-SERVICE/NASA DATA BASE

The Tri-service/NASA data base is being considered at this point because many nonlinear aerodynamic phenomena are illustrated by data from this source. The basic body for the systematic tests consisted of a cylindrical body with an ogive nose 3.0 calibers long for a total body length of 12.5 calibers. A series of fins (fig. 1) ranging in aspect ratio from 0.25 to 4.0 was tested in a tail cruciform arrangement with the body over the angle of attack and Mach number range (shown in fig. 2). The radius to semispan ratio was maintained constant at 0.5. The configurations were all tested over the roll-angle range and, in some of the tests, the fins were deflected as much as ±40° about their hinge lines.

Six component force-and-moment data were taken for the configurations and normal force, root-bending moment, and hinge moment were measured for each fin.

These data form the basis of a prediction method for cruciform missile aerodynamic characteristics, and are incorporated into a code called Missile III (ref. 2). In addition, references 3-5 make use of the Tri-service/NASA data base.

4. WING-BODY INTERFERENCE

Wing-body interference has been an important subject for decades. At high angles of attack it has an effect on the total normal force developed by a missile and its maneuverability. For moderate angles of attack, and subsonic to moderate supersonic Mach numbers methods for predicting interference between midwing and circular bodies are well known. This interference for the wing is measured by a parameter defined by

$$K_{W(B)} = \frac{N_{W(B)}}{N_W} \tag{1}$$

Here $N_{W(B)}$ is the normal force on the undeflected wing divided by the normal force of the wing alone at the same angle of attack. For the normal force carried over onto the body from the wing, an analogous ratio K_B is defined as follows:

$$K_B = \frac{N_{B(W)}}{N_W} \tag{2}$$

The data of the Tri-service/NASA data base are sufficient to see the effect of compressibility on the values of K_W and K_B. In the range of angle of attack and Mach number cited above, both parameters are functions of a/s only. What happens to the value of these parameters at higher values of angle of attack and Mach number has been reported in reference 3 based on the Tri-service/NASA data base.

The value of K_W and K_B/K_W have been extracted from the data base for M_∞ = 2.5, 3.5, and 4.5, and for angles of attack up to 40°. These are tabulated in reference 3 for seven fin planforms varying in aspect ratio and taper ratio. Sufficient information is contained in the reference to determine the normal-force coefficients for the entire configurations.

Plots of K_W versus α are shown in figure 3 for aspect ratio 2 wings as functions of Mach number and taper ratio. The effects of taper ratio are small, but the effects of angle of attack are large. For small angles of attack, K_W tends toward the slender-body value, but at high angles of attack it moves toward one or thereabouts. Thus the favorable body interference on the fins tends to disappear at high angles of attack for all Mach numbers. This result is compatible with the simple method of finding loading on bodies at high angles of attack by using Newtonian impact pressure on all surfaces facing the airstream and assuming vacuum pressure (0) on the leeward surfaces. On page 509 of reference 12 it is seen that the cross-flow Mach number correlates K_W for different Mach numbers.

A series of curves for K_B/K_W is shown in figure 4 in the same format as figure 3. The values of K_B at low α tend generally toward the slender body value of 0.55 or lower. There is a fair amount of scatter in the data. At high

angles of attack ($\alpha \geq 20°$), the value of K_B tends to small values, indicating a loss of lift carryover from the fins to the body for Mach numbers from 2.5 to 4.5.

In connection with the value of K_B/K_W, these values pertain to the short afterbody lengths of the present configuration. These lengths are not uniform. The length of the afterbody probably can have a significant effect on K_B. This problem is a good one for further work, possibly using an Euler code.

Another problem which needs future attention: where is the center-of-pressure location for the lift carryover onto the body from the fin?

5. NONLINEAR CONTROL EFFECT

The control type that will be of interest here is the all-movable control which rotates about a hinge line perpendicular to the body. This information about all-movable controls is also true to a considerable extent about other controls, such as wraparound fins and retractable fins. Extensive measurements were made as a function of M_∞, α, δ, λ, and AR of all-movable fin normal force, root bending moment, and fin hinge moment. Some interesting effects were found in the Tri-service data base as described in reference 4.

Because of the variation in local flow conditions about a body of revolution at high angle of attack as a function of roll angle, the effectiveness of the fin in producing normal force will vary greatly between the leeward and windward fins. The local quantities affecting the fin normal force are the upwash angle, dynamic pressure, and Mach number. As examples of how the effectiveness of a fin in producing normal force varies with M_∞ and ϕ, consider figure 5 (taken from ref. 4). For $\phi = 90°$, the fin is on the windward meridian and for $\phi = -90°$, the fin is on the leeward meridian. Examining the $M_\infty = 4.5$ case first, we note that for constant ϕ, increases in fin deflection from $-40°$ to $+40°$ are always accompanied with increase in fin normal force. At $M_\infty = 2$ there is a peak normal force below $\delta = 40°$ for $\phi > -20°$. Thus there is a fin stall.

A second interesting feature is that at $\phi = 90°$, a given fin deflection produces more change in normal force than it does at $\phi = -90°$. This effect is particularly noticeable at $M = 4.5$ where the fin on the leeward meridian is operating almost in a vacuum.

It is possible to correlate the data of figure 5 by accounting for the local Mach number, dynamic pressure, and upwash angle.* These local quantities are determined by using an Euler code to calculate the body alone flow field. The average value of these quantities over the span of the fin is determined in accordance with the following formula

*The flow angle in a streamwise plane normal to the fin planform.

$$\bar{M}_{\ell} = \frac{1}{s_m - a} \int_a^{s_m} M_{\ell}(\phi,r)dr \tag{3}$$

with analogous formulas for $\bar{\alpha}_{\ell}$ and $\bar{q}_{\ell}$. Using the values of $\bar{M}_{\ell}$ and $\bar{\alpha}_{\ell}$ to define a uniform flow, we find the value of C^*_{NF} in this parallel flow from analysis or wing-alone data. The predicted value of C_{NF} is then given as follows:

$$C_{NF} = C^*_{NF} k_w \frac{\bar{q}_{\ell}}{q_{\infty}} \tag{4}$$

Conversely, the measured value of C_{NF} can be used to calculate k_w. The value of k_w should correlate the fin normal-force data for all roll angles and fin deflections for a given Mach number. Such a correlation is shown in figure 6 by using the data of figure 5. For the $M_{\infty} = 2.0$ results, good correlation is obtained for all the data except the $\delta_2 = +40°$ data near $\phi = 0°$. These data represent a stall condition on the fin as observed in figure 5. For $M_{\infty} = 4.5$, the data correlate well. For ϕ between -90° and -60° the flow is separated, and Euler equation solutions to evaluate $\bar{M}_{\ell}$, $\bar{q}_{\ell}$, and $\bar{\alpha}_{\ell}$ do not give accurate results. Thus k_w is not approximately unity as expected.

The question of hinge moments of all-movable controls at large α and/or large M_{∞} is also of interest. Sufficient data exist in the Tri-service/NASA data base to form the basis of a hinge-moment prediction method. All of the data are for fins having double-wedge sections of varying thickness ratios. A preliminary method for estimating hinge moments at transonic speed is advanced in reference 7.

With regard to pitching moment, knowledge of fin normal force and hinge moment is sufficient to determine the fin contribution to missile pitching moment.

6. TRANSITION AT HYPERSONIC SPEED

Transition from laminar to turbulent flow in missile boundary layers will have large effects on the vortical separated flow field about the missile at high angle of attack, as well as on the heat transfer to the missile itself. It is important to keep in mind that present methods for predicting the location of hypersonic transition can be very inaccurate and this can lead to serious errors in predictions.

Because of the reduced emphasis on hypersonics over the last 15 years, transition research for hypersonic flow has lagged that for lower Mach number flow (ref. 8). There is a significant lack of information on the effects on transition of three-dimensional flow, real gases, shock waves, and pressure gradients. This void must be filled for the design of future hypersonic missiles and aircraft. In the meantime an interim empirical approach to boundary-layer transition at high Mach numbers is suggested in reference 8.

A somewhat fuller discussion on hypersonic boundary-layer transition prediction is given in reference 9. It contains some thoughts on how to predict transition on bodies characterized by a blunt nose, an early frustum, and a frustum.

It is clear that much research must be done before prediction of hypersonic transition can be put on a sound basis. Until reasonable correlation between wind tunnel and flight data at hypersonic speed is achieved, one must be cautious in using wind tunnel data.

7. VORTEX INTERFERENCE

Control problems on missiles caused by vortices can occur in several ways. We first consider the classical case of asymmetric vortex separation on bodies of revolution at high angles of attack, which can occur if the cross-flow Mach number is subsonic. (This is a necessary condition for asymmetric separation, but alone it is not a sufficient one.) A correlation is presented in figure 7 as taken from reference 10 of the maximum side force coefficient caused by asymmetric body vortex separation for bodies of revolution. It can be seen that the asymmetric side force is negligible if the cross-flow Mach number is highly subsonic or supersonic of about $M_c > 0.8$. Asymmetric separation vortices are not to be confused with a Karman vortex strut which can occur with symmetric separation.

A necessary condition for the existence of side force at zero sideslip is that the angle of attack be less than a critical value which depends on Mach number. In figure 8 the region of possible asymmetric side force is indicated. It is noted in figure 7 that bluntness reduces the cross-flow Mach number above which asymmetric side force does not exist.

It is clear that if a nonrolling missile is to operate in a region of vortex asymmetry, the controls must have enough power to handle the side force developed by asymmetric vortices.

Another effect with which the missile controls must cope is vortex switching in which the side force quickly changes sign. It is hoped, however, that this severe requirement can be avoided by making the missile antisymmetric in some way so that vortex switching does not occur. However, means of avoiding vortex switching still need investigation in a wind tunnel which does not have a strong asymmetry itself both for the rolling and nonrolling cases.

The interference associated with symmetric-body vortices still exists at hypersonic speeds. Little is known about the strength and position of vortices at such speeds. For the present, the prediction methods for lower speeds must be used. A combined experimental-theoretical investigation should be made of vortex behavior at hypersonic speeds and large angles of attack. One question of interest is: since density is very low on the leeward surfaces at high α and high Mach number, are the vortex-induced forces significant for body vortex effects or for wing vortex effects on the tail?

It is possible with existing tools to conduct an inquiry into hypersonic vortices, and by using an Euler code, to calculate the entire flow field if the body separation lines are known. This was demonstrated in reference 11 for the symmetric vortices on a body of revolution at $M = 3$ and $\alpha = 15°$. The calculation uses the separation-line position as input and imposes the boundary condition that the velocity vector is tangent to the separation line. To carry out the suggested work requires first determining the body separation lines experimentally for symmetric body vortices at a hypersonic Mach number. One can then carry out the Euler calculations to determine the entire flow field. It can then be seen if the cross-flow field can be well represented by two concentrated vortices using the Biot-Savart law in the cross-flow plane.

One of the variables that might influence the position of the onset of separation is the location of transition, especially at high altitude. The flow condition for the onset of symmetric vortex separation at hypersonic speeds needs to be measured for bodies of revolution. It is not clear that the axial position of separation is necessarily behind the position for the onset of transition so that laminar separation could occur.

Transition at hypersonic speed is thus of possible importance for vortex formation, besides being important for heat transfer.

8. AIRBREATHERS; SUPERSONIC INLETS

Rocket-powered missiles have specific impulses which are a small fraction of those for turbojets, ramjets, or scramjets. Turbojets are limited to a Mach number of about 2 because of the pressure and temperature effects on the rotating structure of gas-turbine engines, whereas the static structures of ramjets and scramjets can stand much higher Mach numbers.

The specific impulse of the power package influences the size and weight of a missile for a given payload and range. The chart of specific impulse versus free-stream Mach number shown in figure 9 (from ref. 12) demonstrates the superiority of ramjets and scramjets for hypersonic missiles. It also depicts the range of operation of the next generation of missiles.

Other than the TALOS and BOMARC, long since out of service, there are no airbreathing tactical missiles in the U.S. military inventory. However, a large amount of research has been done since World War II on airbreathing propulsion for supersonic missile airframes. Because of the reduction in weight and size for a given payload or range, it is strange that more airbreathing missiles have not seen service.

Airbreathing missiles are for the most part of the bank-to-turn kind rather than the rolling kind. If the angle required for the flow to turn into a supersonic inlet at high angle of attack exceeds a certain value (dependent on Mach number), the flow will not turn into the inlet and the inlet will "unstart." For bank-to-

turn missiles putting the inlet on the bottom of the body yields higher inlet pressures as the angle of attack increases. A ramjet is less sensitive to initial flow nonuniformities than is a turbojet engine. Accordingly, a ramjet with the inlet on the bottom surface appears to be a likely candidate for a hypersonic maneuvering missile. The skid-to-turn missile is seen to deteriorate in performance as the angle of attack increases. An example of a ramjet in normal service is the Sea Dart of the Royal British Navy.

In accordance with the purpose of this paper, future problems need to be identified where possible. Inlet technology presents a ripe area for innovation and invention for hypersonic propulsion. One area where future efforts should yield a good payoff is the application of computational fluid dynamics to inlet design. Some preliminary efforts in this direction using an Euler code have been promising. The code also determines the inlet contribution to the stability of the missile.

A few years ago McMillan et al. made a detailed survey of the available information on airbreathing inlets (refs. 13 and 14). The papers contain descriptions of the inlets tested, the testing parameters ranges, and the kinds of measurements made.

9. STORE-SEPARATION PROBLEMS

Many tactical missiles are carried and released by aircraft. During their release they can encounter destabilizing forces and moments caused by the aircraft flow field which can be the most severe in their operating range. A possibility exists of missiles even striking the aircraft.

Most missiles are mounted on external racks and pods and operate well up into the transonic speed range. However, at high transonic speeds they frequently become unstable when released. At supersonic speeds they have so much drag that new methods of carrying and releasing the stores are necessary.

For supersonic aircraft a number of new carriage techniques have been suggested. The methods include mounting the store flush with the bottom of the fuselage (tangential carriage) and semi-submerging the missile in a cutout of the airplane. These methods will significantly reduce the supersonic drag. Another method which has a number of benefits is storing the missile internally to reduce its drag. As an approximation, the missile drag coefficient is the airplane drag coefficient times the internal volume used by the missile divided by the total internal volume of the aircraft, a figure which is a small fraction of the airplane drag. There are no radar cross-section effects created by the missile, except at launching the missile.

The design of cavities for containing missiles at supersonic speeds has been extensively investigated by R. L. Stallings of NASA-Langley (ref. 15). It is important that the cavity not become a Helmholtz resonator when its cover is removed to

separate the missile. This phenomenon is a function of cavity depth-to-length ratio, Mach number, and Reynolds number. Also the pitching moment on the missile should be nose down to have a clear separation of the store from the aircraft. The missile may be given a downward linear velocity and initial angular velocity to aid separation. It is important that a supersonic aircraft be able to separate its missiles at subsonic and supersonic speeds.

Computational fluid dynamics finds use in the study of missile launching from aircraft at both transonic and supersonic speeds. Panel methods can now model complete airplanes. Missiles can also be included in the calculation. In reference 16 Deslandes has applied an Euler code at transonic and supersonic speeds to predict carriage loads on external stores using zonal decomposition. In reference 17, Dougherty, Benek, and Steger apply overlapping grids to solve by iteration for the interference field between several bodies at transonic speed. These authors have just scratched the surface of possibilities for the application of CFD to missile-airplane interference. Much remains to be done. Eventually CFD should largely replace experiment in this application.

While Euler codes give good solutions for many aircraft interference problems, some problems are Reynolds-number dependent so that the Navier-Stokes equations may be called for. Such problems may include missiles at transonic speeds where flow separation occurs because of the close proximity of the stores. Also, open cavities might require the Navier-Stokes equations in certain instances. The field is open for further research.

10. CORRELATION OF MISSILE DATA

While methods exist for calculating the complete flow field about many missile configurations, such calculations are costly and often of unknown accuracy. Engineering prediction methods based on data correlation plus analysis offer a cheaper and faster way of prediction in many cases. Methods for cruciform missiles and planar missiles exist but would benefit from further development.

We now discuss two correlation methods that are useful in engineering prediction methods before describing the methods themselves.

The equivalent angle-of-attack concept (ref. 18) has been very useful in helping to predict the normal force and center-of-pressure location of a fin in the presence of a body. It has also been useful in predicting the amount of normal force carried over onto the body. We will describe the concept here with minimal mathematics and refer the reader to reference 19 for the details.

A fin mounted on a circular body is subject to flow normal to its planform from at least four sources: (a) body angle of attack, (b) fin deflection, (c) sideslip, and (d) vortices. The equation connecting these quantities (without control deflection) is

$$\tan \hat{\alpha}_{eq_i} = K_W \tan \alpha_c \cos \phi_i + \frac{4}{AR} K_\phi \sin \alpha_c \cos \alpha_c \sin \phi_i \cos \phi_i + \tan(\Delta\alpha_v) \quad (5)$$

Adding in control deflection, we have

$$\alpha_{eq_i} = \hat{\alpha}_{eq_i} + \sum_{j=1}^{j=4} \Lambda_{ji} \delta_j$$

where Λ_{ij} is approximately unity for $j = i$ and a small fraction for $j \neq i$. Here $(\Delta\alpha_v^{ij})$ is the average angle of attack induced normal to the fins by the body or other vortices. The basic assumption here in determining the resulting angle of attack of the fin is that the velocities normal to the fin are linearly additive (fig. 10). We do not add component normal forces but use the tangent addition theorem on the component normal velocities. If the normal-force curve of the fin alone is linear, then we could add normal-force components. However, by the present method, nonlinear wing alone normal-force curves can be used. The normal force of the fin in the presence of the body corresponds to that for the wing alone at $\alpha_W = \alpha_{eq}$. Data in reference 20 show excellent correlation of both $C_{N(F)}$ and $(x/c)_F$ versus α_{eq} for data from several sources. Further refinement of Equation (5) considers the induced normal velocity at a given fin caused by the deflections of the other fins through the Λ_{ij} coefficients. It is also possible to linearize Equation (5) and get good results in the moderate angle-of-attack range. An example of the correlation of fin normal force achieved by α_{eq} is shown in figure 11.

The other method of correlation which is useful for missile aerodynamic methods is due to Sychev (ref. 21) as adapted by Hemsch (ref. 6). Hemsch has shown how the modified similarity of Sychev can be used to correlate the normal force and center-of-pressure position for wings and bodies up to high angles of attack, assuming a supersonic cross-flow Mach number.† The normal force and pitching moment for a slender configuration are given by the following set of equations.

$$\frac{C_N}{\sin^2 \alpha} = f_1(k_1, k_2) \quad (6)$$

$$\frac{C_m}{\sin^2 \alpha} = g_1(k_1, k_2) \quad (7)$$

where

$$k_1 = \frac{b/\ell}{\tan \alpha} \qquad k_2 = M_\infty \sin \alpha \quad (8)$$

Introducing a third parameter

$$k_3 = \frac{\tan \alpha}{AR} = \frac{\text{constant}}{k_1} \quad (9)$$

†This assumption turns out to be unnecessary for some reason.

the normal-force coefficient and center-of-pressure location turn out to be

$$\frac{C_N}{AR \sin \alpha \cos \alpha} = f_2(k_2,k_3) \tag{10}$$

$$\frac{\bar{x}}{\ell} = g_2(k_2,k_3) \tag{11}$$

Hemsch applied the results to a systematic series of sharp delta wings tested by Miller and Wood‡ (ref. 22). He first plotted the position for the various data points in the k_2,k_3 plane as shown in figure 12. Four regions were found which corresponded to four types of delta-wing flow. It is then shown that two fins with the same values of k_2 and k_3 yield the same pressure coefficients in the form $C_p/\sin^2 \alpha$ versus y/s. This assumes similar airfoil shapes.

A simplification was found for the wings of the Stallings-Lamb data (ref. 23) consisting of wings varying in aspect ratio from 0.25 to 4.0 and with taper ratios of 0, 0.5, and 1.0. An accurate data correlation was found in the form

$$\frac{C_N}{AR \sin \alpha \cos \alpha} = A \left(\frac{\tan \alpha}{AR} \right)^B \tag{12}$$

where

$$A = A(M_\infty \sin \alpha) \; ; \qquad B = B(M_\infty \sin \alpha) \tag{13}$$

Hemsch found that three families of sharp-edged wings and two families of smooth bodies had normal force curves as represented by equations (12) and (13). It was also possible to correlate the center-of-pressure position of wings alone as curves of $\bar{y}/s$ versus α/AR with $M_\infty \sin \alpha$ as a parameter.

11. CFD CODES FOR COMPLETE CONFIGURATIONS

It is often of interest to calculate the pressure or flow field for a complete missile or for a missile in the presence of an airframe. Various codes exist in the United States for this purpose. The codes vary in their speed, range of applicability, and the partial differential equation being solved among other ways. Four codes are compared in figure 13. These four codes are: (1) PANAIR (ref. 24), (2) TRANAIR (ref. 25), (3) DEMON (ref. 26), and (4) SWINT (ref. 27).

PANAIR (ref. 24) is a code intended to solve the linear aerodynamic theory (the Glauert-Prandtl equation) for complete configurations of some complexity. Although developed for airplane use, it can easily be adapted to a missile in flight. It can also handle a separating missile still within the influence of the airplane.

PANAIR can be used through the subsonic and supersonic speed range except in the nonlinear transonic range. For this purpose, TRANAIR was created for application to aircraft in the nonlinear transonic region (ref. 25). It is applicable to missiles. The code solves the full potential equation for the entire flow field. It can be adapted to apply to an airplane-store combination.

DEMON (ref. 26) is a supersonic panel program based on the Glauert-Prandtl rule. However, nonlinear compressibilities effects are accounted for in an engineering approximation. It handles both body and fin vortices, and it is applicable when calculating interference between missiles and airplanes.

Finally, SWINT (ref. 27) is a supersonic marching code based on the Euler equations. It employs a grid with radial lines from a center somewhere in the body. The radial lines in the cross-flow plane are allowed to intersect the surface of the missile only once. This limits its application to a class of missile configurations. The important aspect of SWINT is that it is based on the Euler equations which handle nonlinear compressibility effects precisely.

There are gaps in the application of the foregoing codes. The difficulty in some cases, which is due to the mesh of the Euler code just discussed, can be overcome, and this problem is a good one for future work. At the same time, it might also be modified to handle multiconnected regions. If the Mach number in the marching direction becomes subsonic, the Euler code "blows up" (this usually occurs at some limiting angle of attack). A method for handling small regions of embedded subsonic flow with the Euler equation would be of interest.

All the codes have been or can be adjusted to account for vortices in an engineering fashion. The rigorous treatment of the vortices awaits a Navier-Stokes code to handle the vortices from first principles. There are a number of Euler solvers besides SWINT for solving flow problems of supersonic missiles.
In fact, four different Euler solvers have been compared by Priolo, Wardlaw, and Solomon in reference 28. SWINT has a number of shortcomings including geometric limitations, occasional instability in calculation, use of special means at leading edges, trailing edges and tips, inability to reproduce sharp shock discontinuities, and use of artificial viscosity. MUSE is an extension of SWINT to handle fin thickness and more general geometrics. ZEUS E is a first-order code using the Gudonov method while ZEUS H is a second-order code using the Gudonov method. The Gudonov method can remove most of the instabilities occurring in SWINT. It does not need artificial viscosity nor special procedures; it gives sharp discontinuities associated with shocks. While these advances improve Euler codes, further advances are needed to handle viscous effects in a rotational inviscid way.

A supersonic panel code has been coupled with a NASTRAN code to determine static aeroelastic forces and moments as well as deformed shapes. This work has been accomplished by Dillenius et al. and is reported in reference 29. The combined program has been provided with an optimizing capability. One application under consideration is how to design a fin to minimize hinge moments. McIntosh and

[‡]Miller and Woods obtained similar results using different parameters.

Dillenius have written an aeroelastic tailoring procedure for reduction of fin hinge moments. The code (ref. 30) makes use of McIntosh and Dillenius' DEMON code.

12. ENGINEERING PREDICTION METHODS

It is not economical and, in certain cases, not currently possible to calculate the aerodynamic characteristics of complete tactical missiles using CFD. Therefore, much preliminary design is done by engineering prediction methods. Many companies have their own engineering-prediction methods which are not in the public domain. However, there are several engineering methods that are in the public domain and which we will discuss: (a) MISSILE DATCOM (ref. 31), (b) MISSILE III (ref. 32), and (c) Schindel's Code (ref. 33).

We are discussing MISSILE DATCOM for purposes of completeness and comparison. MISSILE DATCOM is a collection of empirical, semiempirical, and theoretical methods mostly applicable to ordinary missiles. An "ordinary" missile is defined as either a planar or cruciform missile with an axisymmetric body. Two pairs of fins are included which are in line or are interdigitalized by 45°. We will not discuss the methodology which is described in reference 31.

MISSILE DATCOM was used to predict the coefficients C_N, C_M, and C_A for a large number of missile configurations. The tolerances allowable in the predictions were:

C_N: ±20%

C_M: ±20% or 25% L

C_A: ±10% or ±2 $C_D/C_A \cos \alpha$

At $\alpha \leq 20°$, the method fell within the tolerances 60% of the time; for $\alpha \leq 40°$, 40% of the time. Clearly the method is not a high-α method. For closely coupled wings and tails, it does not handle wing-body interference well; however, this matter can be rectified. It is not well adapted to handling α-δ coupling of all-movable fins or to handling asymmetric ϕ settings well, or the effects of α and M on K_B and K_W. Reference 3 gives systematic data sufficient for updating the effects of α and M on K_W and K_B.

The next computer code, MISSILE III, supplements DATCOM in some instances. It utilizes a newly available systematic Tri-service/NASA data base previously described. It covers the Mach range 0.6 to 4.5, fin aspect ratio from 0.25 to 4.0, angles of attack up to 45°, and arbitrary roll angles. It contains also a set of data for systematic variations of ϕ and δ, for a number of fins over an α and M range. These data are sufficient to handle α-δ coupling as well as δ_i-δ_j coupling, assuming this latter quantity is small. The program's disadvantage is that it does not handle drag.

The data were taken at $a/s = 0.5$. For $a/s = 0$ there is no wing-body interference so that $K_W = 1$ and $K_B = 0$. For other a/s ratios, a linear interpolation is made between $a/s = 0$ and 0.5 for K_W and K_B as is approximately true from slender-body theory. This assumption has never been clearly investigated and would be a worthwhile subject of future research. The generalization of $a/s = 0.5$ data to any a/s gives the data base an additional parameter of freedom. Also the effects of putting a wing and tail on a missile are handled by providing a wing-tail interference method in the program. In these ways, the applicability of the data base is vastly expanded.

It is clear that anything that can be accomplished with MISSILE III could also be added to MISSILE DATCOM.

A number (6) of suggestions for the extension of MISSILE III are included in reference 32.

In reference 33 Schindel has produced a computer code for preliminary design and screening of missile airframes. Its virtues are that it is fast and applicable to waveriders. It also includes a plotting routine for the results.

13. SOME FUTURE CONFIGURATIONS

As a result of future trends in tactical missiles, a number of new concepts are being advanced to fill the needs. These configurations include waveriders, noncircular bodies, airbreathing engines, etc. We will examine a number of these future configurations.

Consider first the waverider which is now receiving much attention. Figure 14 illustrates a waverider at its design point. It is the type of waverider known as a caret wing. Its upper surface consists of two triangular planes joined at a hinge line. At the design condition, the hinge line is parallel to the freestream direction, and no pressure exists on the upper surfaces. In the chordwise direction, the airfoil sections are all wedge sections of a uniform wedge angle. The flow under the wing is all parallel flow at oblique shock pressure. The region between the bottom of the waverider and a plane containing the apex and wing tips is at uniform pressure. We thus know its lift/drag ratio from oblique shock theory. Waveriders have higher L/D ratios at hypersonic speeds than the usual cruciform missiles by about a factor of 2. Waveriders were seriously considered for designs of hypersonic aircraft by Kucheman (ref. 34) and his associates in England about 25 years ago. It is only recently that waveriders have been given serious attention for hypersonic tactical missiles.

A large variety of waverider configurations is possible (Schindel, ref. 35). The use of waveriders as missiles presents a series of aerodynamic problems such as adding a propulsion system, controls, and a radome to the basic waverider, hopefully without seriously degrading $(L/D)_{max}$. It is clear that considering the large number

of waverider configurations and the above aerodynamic problems, a large and fruitful opportunity exists for research and development in this field.

An interesting study in the optimization of hypersonic waveriders is given in reference 36. In this study, a class of waveriders was optimized for maximum L/D ratio considering skin friction and blunt leading-edge drag. At $M = 6$ an L/D over 8 was calculated and at $M = 25$ an L/D of about 4.5 was calculated.

One virtue of the conical waverider is that its center of pressure remains constant at supersonic speed as long as the flow is attached. Of interest is how much the L/D is degraded by adding the necessary components to make it into an airplane.

With the introduction of airbreathing missiles to achieve range, it becomes possible to use noncircular bodies which do not roll continuously. This possibility opens up the design space and allows increased performance and increased stability and control. While rocket powered cruciform missiles usually use skid-to-turn maneuverability, airbreathers utilize bank-to-turn maneuvering. Possible advantages claimed in the use of noncircular bodies include higher lift, better storage, improved carriage, better separation, and improved stability and control.

A nonplanar missile on a noncircular body represents an interesting new design possibility which can have different stability and control than the usual cruciform missile. A few examples with noncircular bodies are now presented.

A circular body can develop rolling moments by skin friction but they are of small magnitude. It thus has zero effective dihedral, C_{ℓ_β}. A noncircular body under sideslip can have rolling moment and side force as a result of pressure forces, yielding finite values of C_{ℓ_β} and C_{n_β}. Figure 15 shows the effective dihedral and directional stability of an elliptical body as compared to a circular one of the same area distribution. Note that the elliptical body has good effective dihedral while the circular body has neutral stability. Both bodies have poor directional stability, but the elliptical body is less unstable than the circular body and will thus require a smaller vertical fin.

Many investigations have advanced configurational ideas for improved hypersonic missiles (refs. 37-39). A number of these configurations discussed in reference 37 have flat tops and are presented in figure 16. The maximum L/D ratios are presented there for both flat top and flat bottom orientations. The difference in maximum L/D between the two orientations is not very large. It is thus possible to provide volume below the wing to house the engine. Also, the positive pressure gives the engine more thrust. The maximum L/D ratios shown in figure 16 are below the empirical limit given by Kucheman in reference 34.

$$\left(\frac{L}{D}\right)_{max} = \frac{4(M + 3)}{M} \tag{14}$$

The stability and control characteristics of monoplanes with elliptical bodies generally provides a good balance between longitudinal and lateral-directional stabilities. Too low a profile, looking normal to the body in the horizontal plane,

reduces the directional stability. It also causes unporting of controls at high deflections with an attendant loss of control.

Hunt and his coworkers (ref. 38) have studied hypersonic missile airframes capable of housing a scramjet engine. The studies showed engine/airframe integration to be a significant problem for this class of missiles. Also the engine can have a significant effect on the missile's stability and control. In reference 39 Spearman analyzes the aerodynamics of some unconventional missiles and considers their applicability to certain missions. The classes of missiles considered are: (1) delta-wing bodies (fig. 17), (2) ring-parasol wing bodies (fig. 18), and (3) monoplanar missile with circular/elliptical body (fig. 19). Spearman's objective was to indicate the types of mission suitable for various configurations. The requirements for various missions include full load carrying capability, low drag, low detectability, ease of carriage and stowage, low cost, etc.

Spearman's candidate for a tactical penetrator capable of high speed, low-altitude overflight with downward spray of warhead fragments is the thick delta wing and a semi-conical body with delta wings. This configuration, being small and slender, is hard to detect. High-speed, high-altitude concepts with good aerodynamic efficiency for volume and range are a possible approach to strategic penetration. The parasol wing concept appears to be applicable to this mission. It provides high-lift capability at low angle of attack by utilizing favorable interference flow fields.

A monoplanar wing in connection with an elliptical body is a good candidate for a maneuvering missile such as required in air defense or air combat missions. Its high L/D makes it a good candidate for longer range air-to-surface missions.

In this section we have considered four general categories of missile types: (a) waveriders, (b) flat-top monoplanar missiles, (c) missiles designed for scramjet propulsion, and (d) missiles suitable for particular missions. Although a number of stability and control problems have been mentioned in connection with these missile types, a great amount of research and development will be required in the future.

A detailed discussion of waveriders is to be found in reference 35 and of bank-to-turn missiles with noncircular bodies in reference 40.

14. CONCLUDING REMARKS

In this paper a wide range of subjects in missile aerodynamics has been covered from a general point of view. Certain subjects such as aerodynamic heating, drag, radar cross-section, and real gas effects have been neglected because of space limitations or classification restrictions. The first two subjects are well covered by chapters IX and X in the book "Tactical Missile Aerodynamics," Vol. 104, AIAA Series Progress in Astronautics and Aeronautics.

15. ACKNOWLEDGMENT

I am grateful to Dr. Michael Hemsch, who reviewed the document and made a number of helpful suggestions.

REFERENCES

1. "Missile Aerodynamics," AGARD-CP-336, Restricted NATO, presented at the Fluid Dynamics Panel Symposium, Sept. 20-22, 1982, Trondheim, Norway.

2. Lesieutre, D. J., Mendenhall, M. R., Nazario, S. M., and Hemsch, M. J., "Aerodynamic Characteristics of Cruciform Missiles at High Angles of Attack," AIAA Paper 87-0212, 1987.

3. Nielsen, J. N., "Supersonic Wing-Body Interference at High Angles of Attack with Emphasis on Low Aspect Ratios," AIAA Paper 86-0568, 1986.

4. Hemsch, M. J. and Nielsen, J. N., "Extension of Equivalent Angle-of-Attack Method for Nonlinear Flow Fields," J. Spacecraft and Rockets, Vol. 22, No. 3, pp. 304-308, May-June 1985.

5. Lesieutre, D. J., Mendenhall, M. R., Nazario, S. M., and Hemsch, M. J., "Prediction of the Aerodynamic Characteristics of Cruciform Missiles Including Effects of Roll Angle and Control Deflection," NEAR TR-360, 1987.

6. Hemsch, M. J., "Engineering Analysis of Slender-Body Aerodynamics Using Sychev Similarity Parameters," AIAA Paper 87-0267, 1987. (To be presented in J. Aircraft, 1988.)

7. Nielsen, J. N., Goodwin, F. K., and Dillenius, M. F. E., "Prediction of Cruciform All-Movable Control Characteristics at Transonic Speeds," NEAR TR-321, 1984.

8. Reshotko, E., Bushnell, D. M., and Cassidy, M. D., "Report of the Task Force on Boundary Layer Transition," NASP TM-1007, 1987.

9. Stetson, K. F., "On Predicting Hypersonic Boundary Layer Transition," AFWAL-TM-87-160-FIMG, March 1987.

10. Wardlaw, A. B., Jr. and Morrison, A. M., "Induced Side Forces at High Angles of Attack," NSWC/WOL/TR 75-17, 1975.

11. Klopfer, G. H. and Nielsen, J. N., "Euler Solutions of the Body Vortices of Tangent Ogive Cylinders at High Angles of Attack and Supersonic Speeds," AIAA Paper 81-0361, 1981. Also NEAR TR-130.

12. Tactical Missile Aerodynamics, Progress in Astronautics and Aeronautics, Vol. 104, Martin Summerfell, Series Editor in Cheif, Chapter 4, Inlets, by A. N. Thomas, Jr., the Marquandt Co., Van Nuys, Calif., pp. 129-167.

13. McMillan, O. J., Perkins, S. C., Jr., Perkins, E. W., and Kuhn, G. D., "Data Base for the Prediction of Airbreathing Missile Airframe/Propulsion System Interference Effects (U)," NWC TP-6136, 1980, Limited Distribution. (Prepared under Contract N60530-78-C-0098 (Confidential Report).)

14. Perkins, Stanley C., Jr. and McMillan, O. J., "A Handbook of Experimental Data for the Effects of Inlet Systems on Airbreathing Missile External Aerodynamics (U)," NWC TP-6147, 1982, Limited Distribution. (Prepared under Contract N60530-78-C-0201.) Vol. 1, Overview and Summary (U) (Confidential); Vol. 2, Configuration Data: Inlet Type Effects (U) (Unclassified, but Limited Distribution); Vol. 3, Data Classified by Inlet Type, Part 1 (U) (Confidential); Vol. 3, Data Classified by Inlet Type, Part 2 (U) (Confidential).

15. Stallings, R. L., "Store Separation from Cavities at Supersonic Flight Speeds," Journal of Spacecraft and Rockets, Vol. 20, pp. 129-132, March-April 1983.

16. Deslandes, Ronald, "Zonal Decomposition: An Advanced Concept for Euler Codes in Order to Predict Carriage Loads of Non-Trivial External Store Configurations," Paper No. 2, AGARD CP-389, 1986.

17. Dougherty, F. C., Benek, J. A., and Steger, J. L., "On the Application of Chimera Grid Schemes to Store Separation," AGARD CP-389, 1986.

18. Smith, C. A., Nielsen, J. N., and Hemsch, M., "Prediction of Aerodynamic Characteristics of Banked Cruciform Missiles at High Angles of Attack," AIAA Paper 79-0024, 1979.

19. Hemsch, M. and Nielsen, J., "The Equivalent Angle-of-Attack Concept for Engineering Analysis," Chpt. XI, "Tactical Missile Aerodynamics," Vol. 104, Progress in Astronautics and Aeronautics, AIAA, 1986.

20. Hemsch, M. J. and Nielsen, J. N., "Equivalent Angle of Attack Method for Estimating Nonlinear Aerodynamics of Missile Fins," J. Spacecraft and Rockets, Vol. 20, pp. 356-362, July-August 1983.

21. Sychev, V. V., "Three-Dimensional Hypersonic Gas Flow Past Slender Bodies at High Angles of Attack," J. Appl. Math. and Mech., Vol. 24, pp. 286-306, 1960.

22. Miller, R. S. and Wood, R. M., "Leeside Flow Over Delta Wings at Supersonic Speeds," NASA TP-2430, 1985.

23. Stallings, R. L., Jr. and Lamb, M., "Wing-alone Aerodynamics Characteristics for High Angles of Attack at Supersonic Speeds," NASA TP-1889, 1981.

24. Derbyshire, T. and Sidwell, K. W., "PANAIR Summary Document," NASA CR-3250, 1982.

25. Samant, S. S., Bussoletti, J. E., Johnson, F. T., Burkhart, R. H., Everson, B. L., Melvin, R. G., Young, D. P., Erickson, L. L., Madson, M. D., and Woo, A. C., "TRANAIR: A Computer Code for Transonic Analysis of Arbitrary Configuration," AIAA Paper 87-0034, 1987.

26. Dillenius, Marnix F. E., "Aerodynamic Predictions Using Supersonic Paneling Methods Accounting for Vorticity and Nonlinear Effects," AIAA Paper 86-0569, 1986.

27. Wardlaw, A. B., Priolo, F. J., and Solomon, J. M., "A Multiple-Zone Method for Supersonic Tactical Missiles," NSWC TR 85-484, 1986.

28. Priolo, F. J. and Wardlaw, A. B. Jr., "A Comparison of Inviscid Computational Methods for Supersonic Tactical Missiles," AIAA Paper 87-0113, 1987.

29. Dillenius, M. F. E., Perkins, S. C., Jr., and Lesieutre, D. J., "Modified NWCDM-NSTRN and Supersonic Store Programs for Calculating NASTRAN Forces Acting on Missiles Attached to Supersonic Aircraft," NEAR TR 369, 1987.

30. McIntosh, S. C., Jr. and Dillenius, M. F. E., "Aeroelastic Tailoring Procedure for Reduction of Fin Hinge Moments," NEAR 374, 1987.

31. Vukelich, S. R. and Jenkins, J. E., "MISSILE DATACOM: Aerodynamic Predictions of Conventional Missiles Using Component Build-up Techniques," AIAA Paper 84-0388, 1984.

32. Lesieutre, D. J., Mendenhall, M. R., Nazario, S. M., and Hemsch, M. J., "Prediction of the Aerodynamic Characteristics of Cruciform Missiles Including Effects of Roll Angle and Control Deflection," NEAR TR-360, 1986.

33. Schindel, L. H., "A Preliminary Design and Screening Process for Missile Airframe Configurations," AIAA Preprint 87-0211, 1987.

34. Kucheman, D., The Aerodynamic Design of Aircraft, Pergamon Press, Oxford, pp. 448-510, 1978.

35. Schindel, L., Waveriders, Chpt. 6 in "Tactical Missile Aerodynamics," AIAA Progress in Astronautics and Aeronautics, Vol. 104, 1986.

36. Bowcutt, K. G., Anderson, J. D., and Capriotti, D., "Viscous Optimized Hypersonic Waveriders," AIAA Paper 87-0272, 1987.

37. Krieger, R. J., Gregoire, J. E., Hood, R. F., Eiswirth, E. A., and Taylor, M. L., "Aerodynamic Configured Missile Development--Final Report," Vols. 1-5, AFWAL-TR-80-3071, 1980.

38. Hunt, J. L., Johnston, P. J., Cubbage, J. M., Dillon, J. L., Richie, C. G., and Marcum, D. C., Jr., "Hypersonic Airbreathing Missile Concepts Under Study at Langley," AIAA Paper 82-0316, 1982.

39. Spearman, M. L., "Unconventional Missile Concepts from Consideration of Varied Mission Requirements," AIAA Preprint 84-0076, 1984.

40. Jackson, C. M., Jr. and Sawyer, W. C., "Bodies with Noncircular Cross Sections and Bank-to-Turn Missiles," Chpt. V, pp. 168-187, in "Tactical Missile Aerodynamics," Vol. 104 in AIAA Series "Progress in Astronautics and Aeronautics."

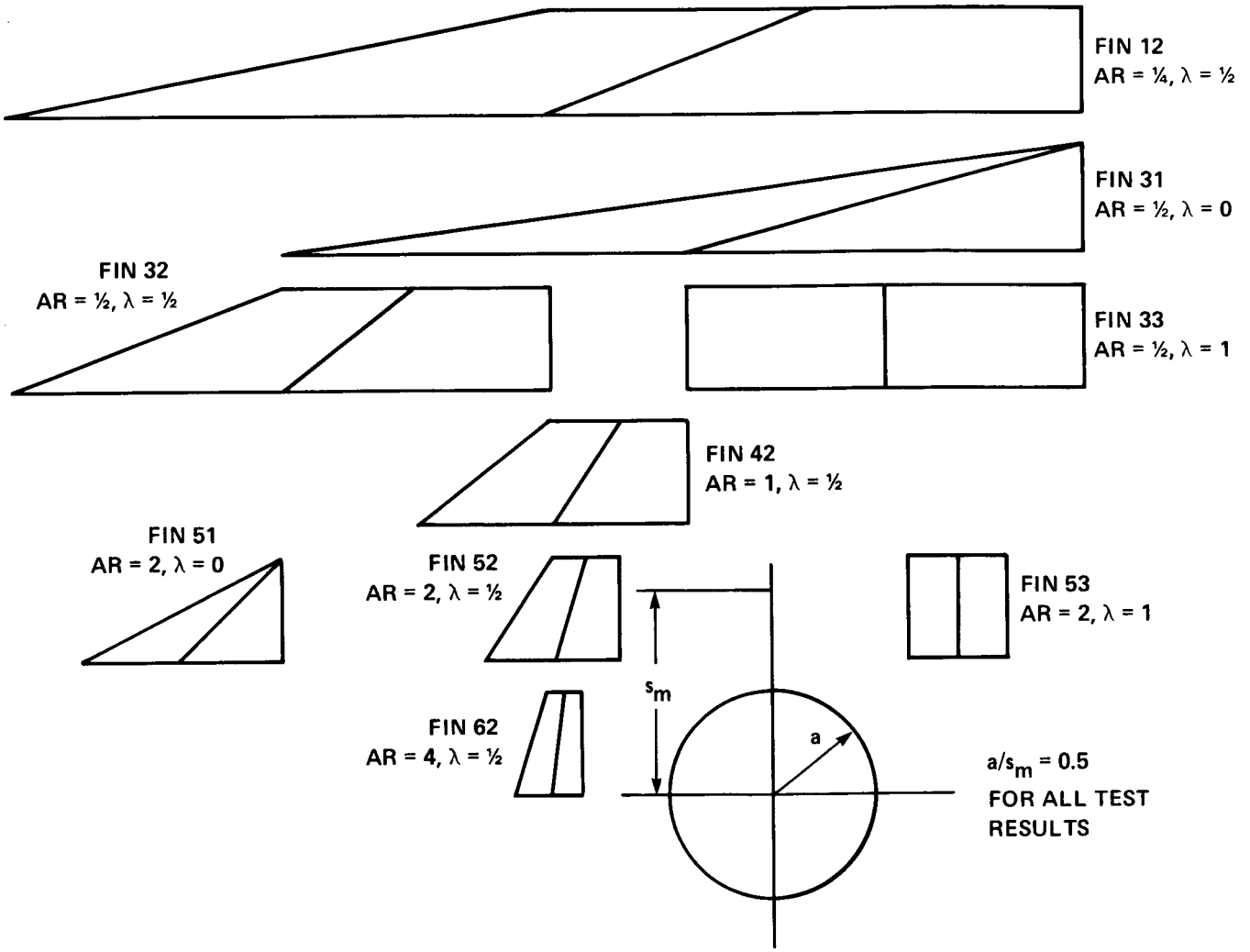

Figure 1.- Test fin geometrics.

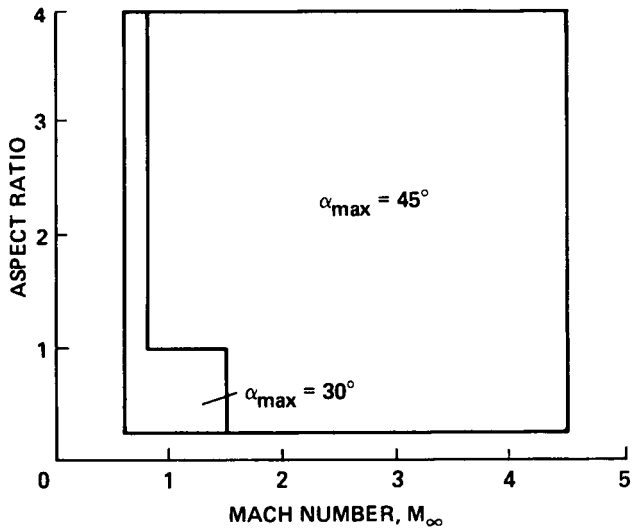

Figure 2.- Mach number and aspect ratio ranges and maximum angle of attack for Tri-service data base.

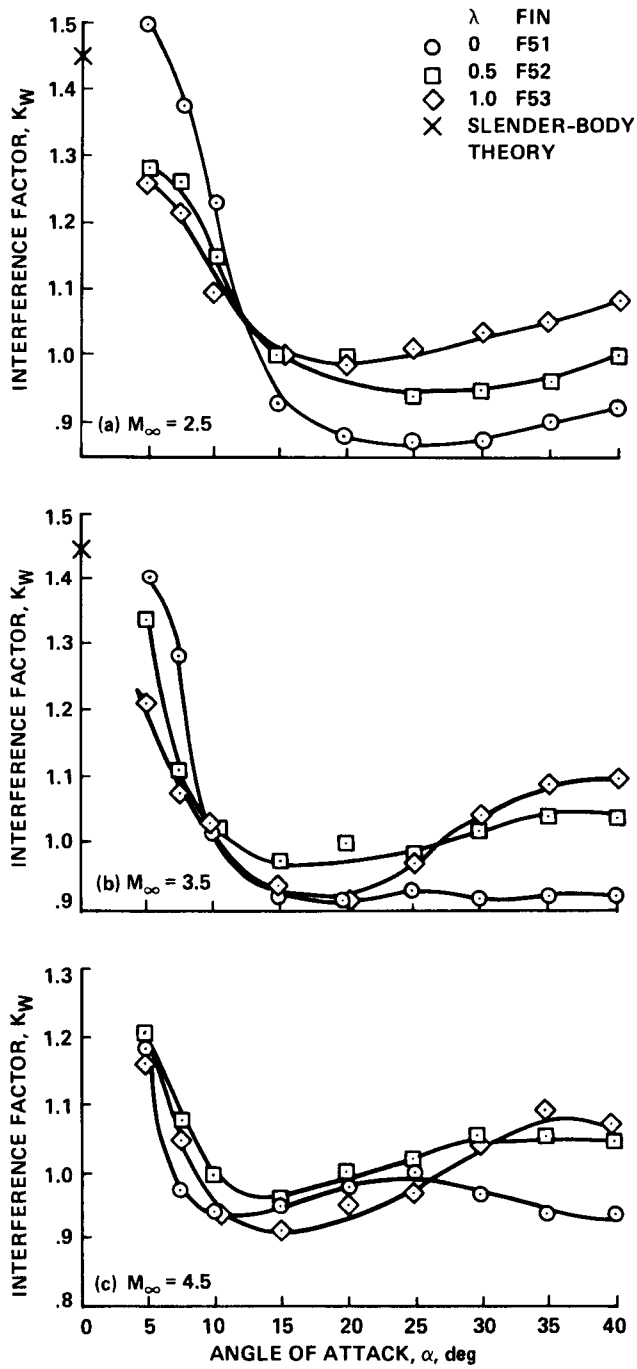

Figure 3.- Effect of taper ratio on interference factor K_W for aspect ratio 2 fins.

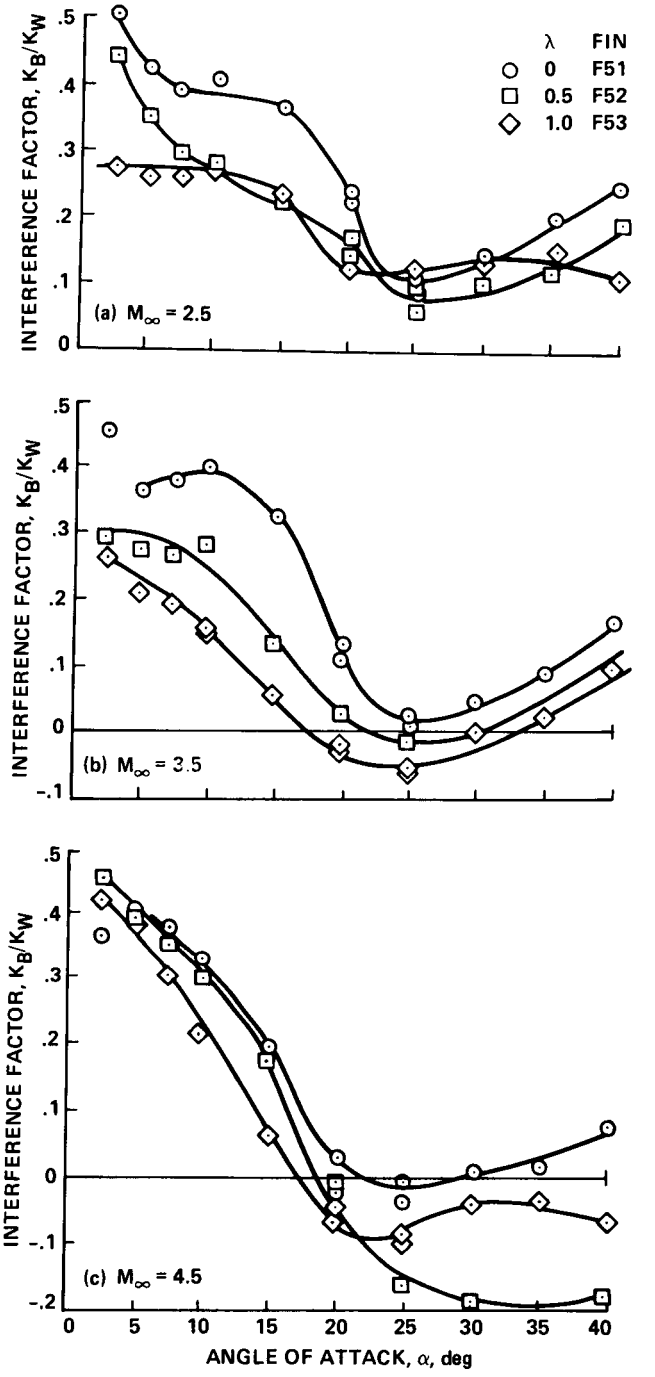

Figure 4.- Effect of taper ratio on K_B/K_W for aspect ratio 2 fins.

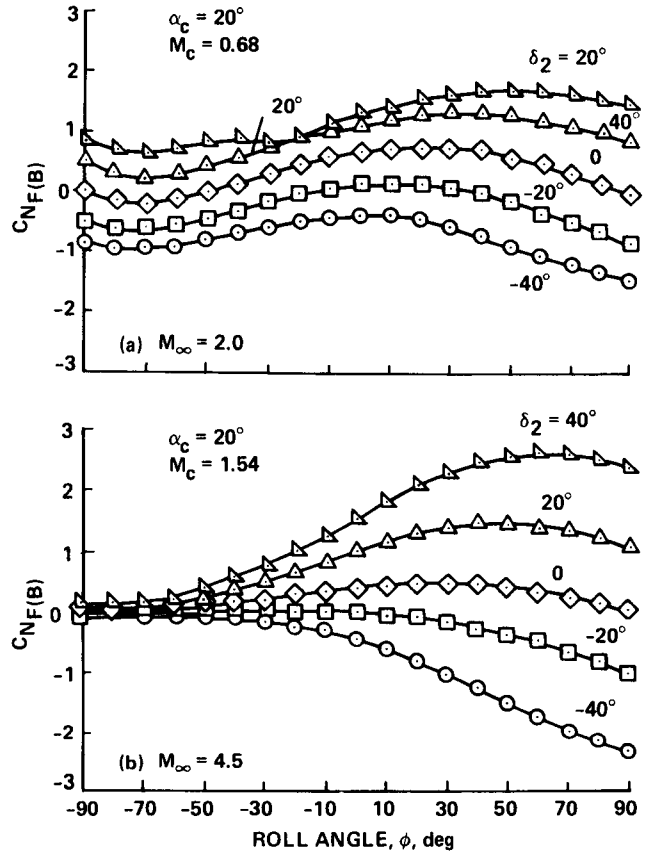

Figure 5.- Effect of roll angle and fin deflection on the normal force generated by fin F2.

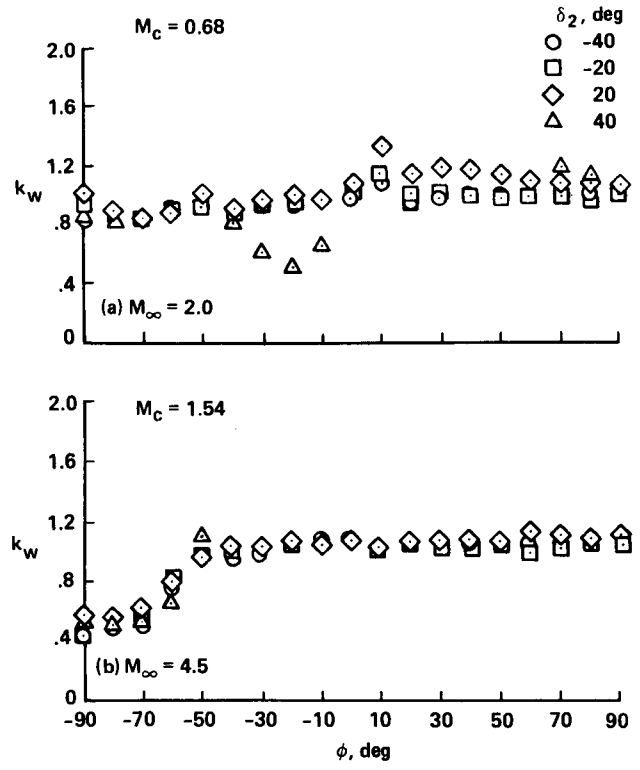

Figure 6.- Effect of roll angle and control deflection on k_w for all-movable controls.

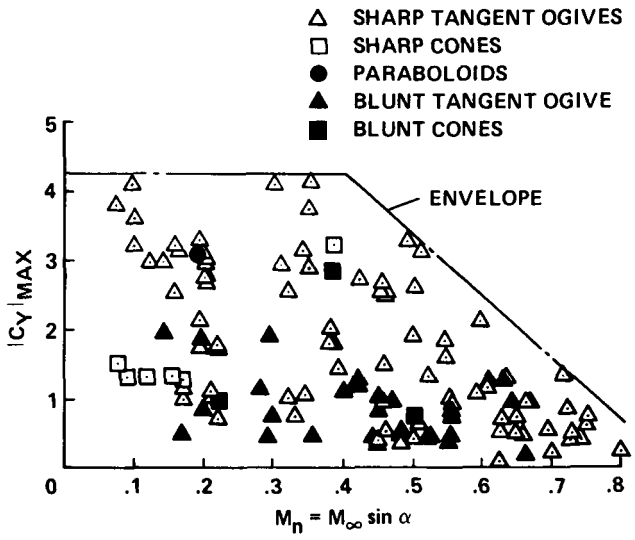

Figure 7.- Effect on crossflow Mach number on the sideforce of cones, tangent ogives, and paraboloids.

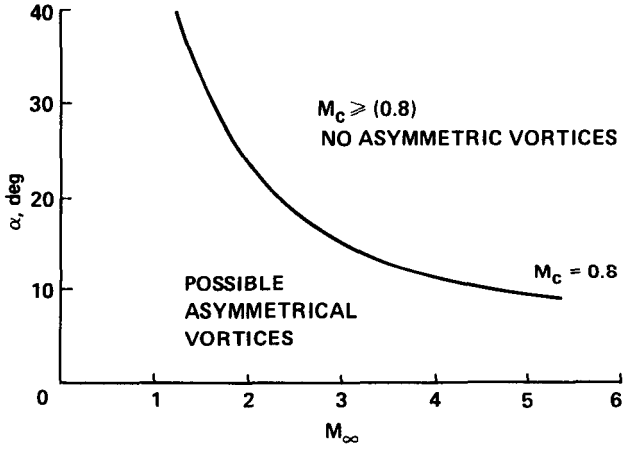

Figure 8.- Boundary between symmetric separation and asymmetric separation for body of revolution.

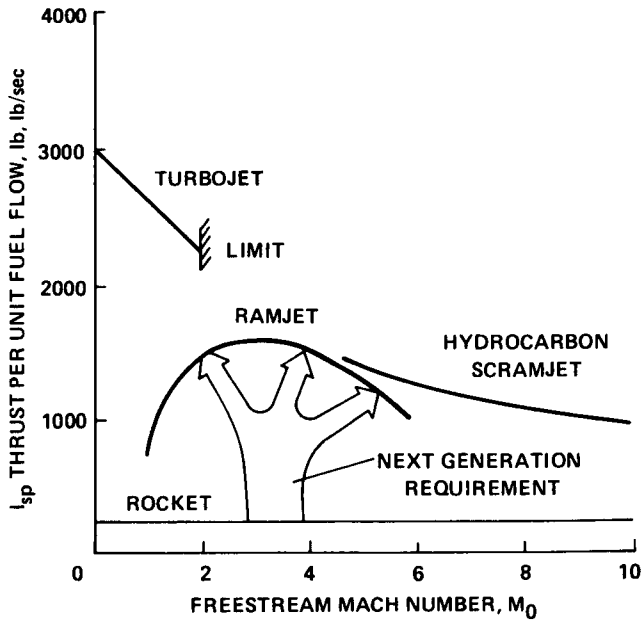

Figure 9.- Specific thrusts of various propulsion means.

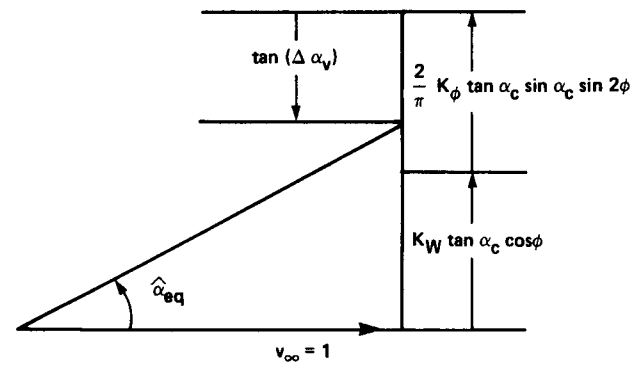

Figure 10.- Addition of velocity components normal to fin defining equivalent angle of attack.

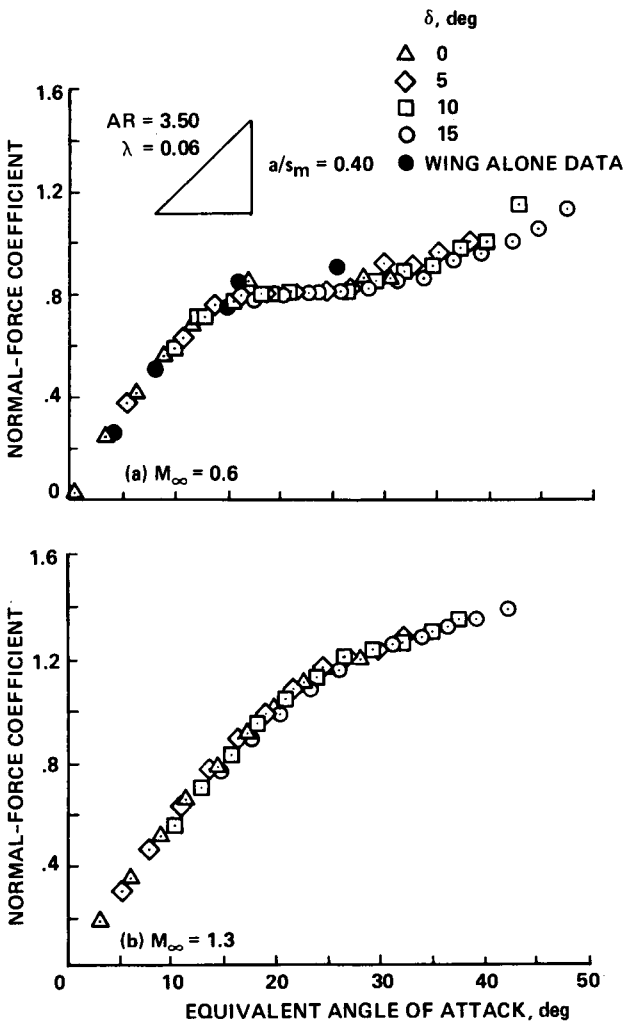

Figure 11.- Correlation of normal force coefficients with the equivalent angle of attack for moderate aspect ratio fin.

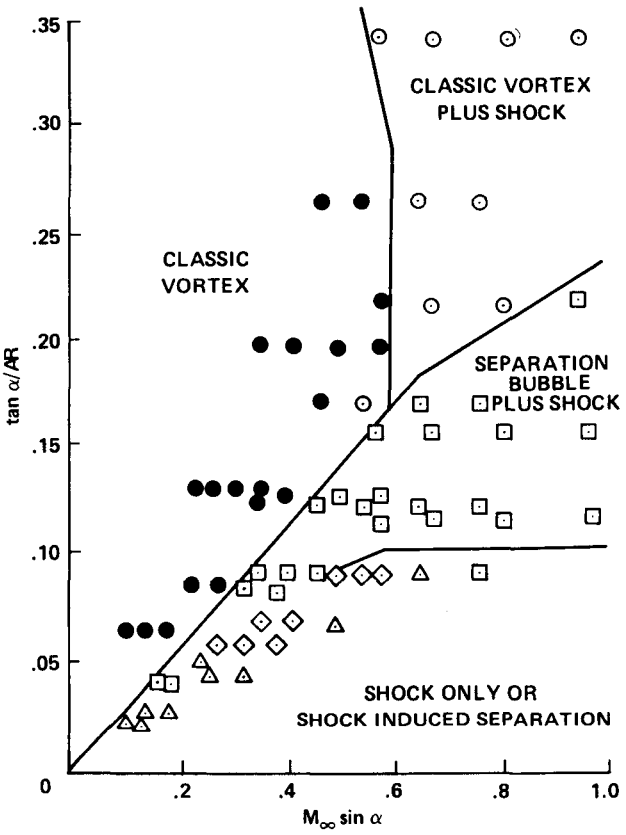

Figure 12.- Classification of Miller-Wood delta wing flow field data using the Sychev similarity parameters.

	PANAIR	TRANAIR	DEMON III	SWINT
PANEL OR FIELD	PANEL	FIELD	PANEL	FIELD
BASIC EQUATION	GLAUERT – PRANDTL	FULL POTENTIAL	GLAUERT – PRANDTL	EULER
MACH NUMBER RANGE	-0.9 1.2–2.5	0.6–0.95	$M \geqslant 1.1$	$M > 1$
BODY VORTICES	NO	NO	YES	NO
WING-TAIL INTERFERENCE	MUST INPUT VORTEX POSITION	MUST INPUT VORTEX POSITION	YES	?

Figure 13.- Characteristics of computer codes for calculating the loading on missiles or aircraft.

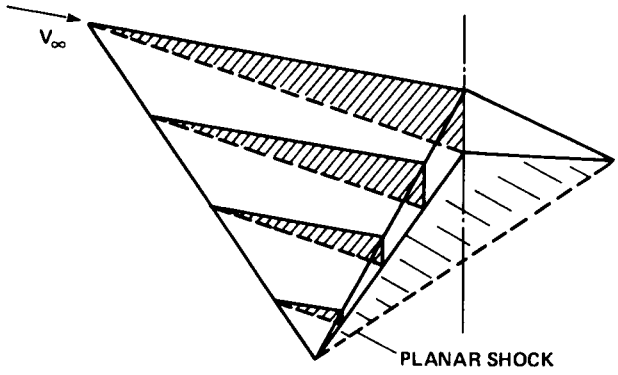

Figure 14.- Sketch of a simple waverider, a caret wing.

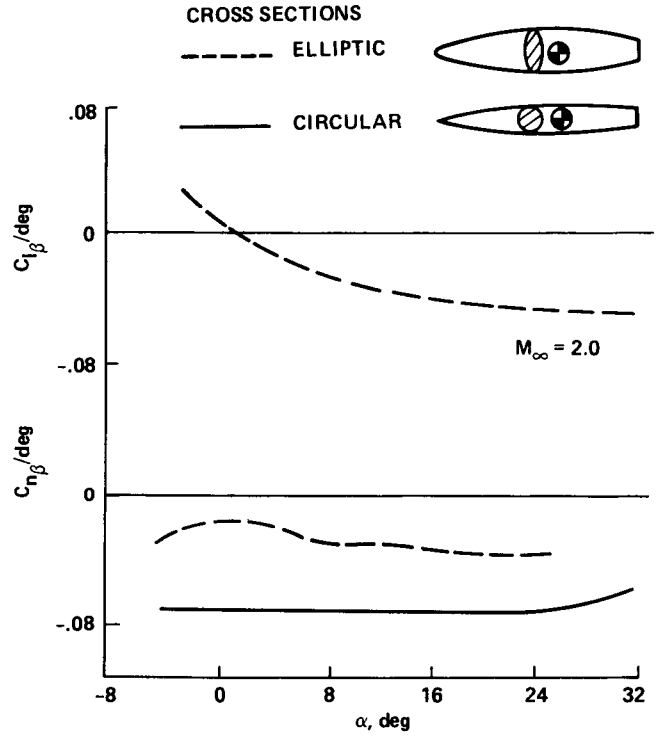

Figure 15.- Comparisons of effective dihedral and directional stabilities between Sear-Haack bodies of circular and elliptical cross section.

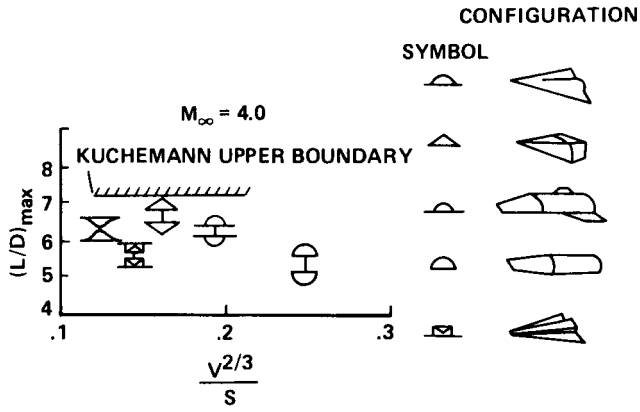

Figure 16.- Shape effects on maximum lift-drag ratios both right side up and upside down.

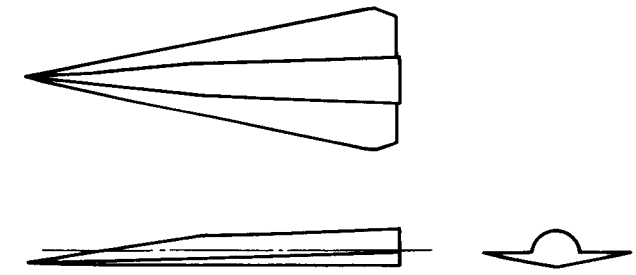

(a) SEMICONICAL BODY WITH DELTA WINGS

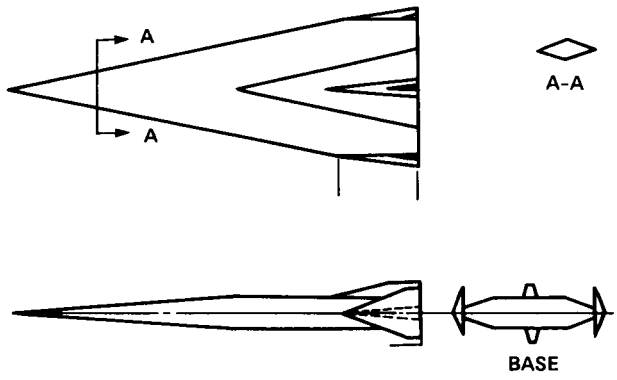

(b) THICK DELTA WING CONCEPT

Figure 17.- Some delta wing-body concepts of Spearman.

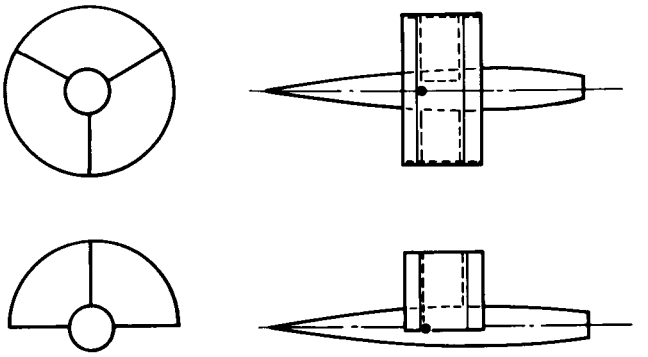

(a) RING-WING-BODY CONCEPTS

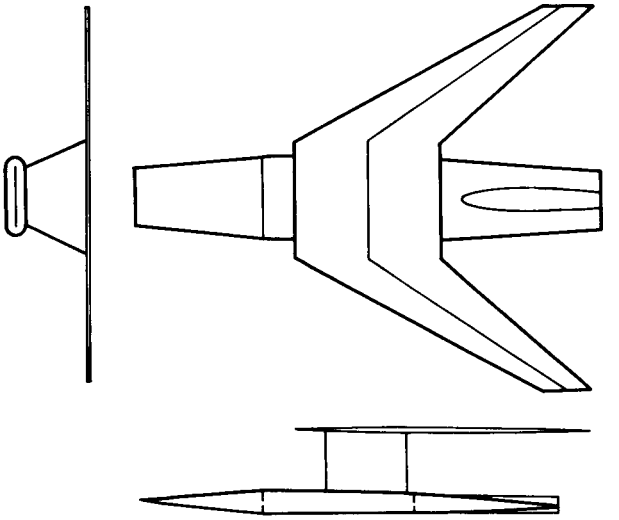

(b) FLAT BODY WITH SWEPT PARASOL WING

Figure 18.- Ring wing-body and parasol wing-body concepts of Spearman.

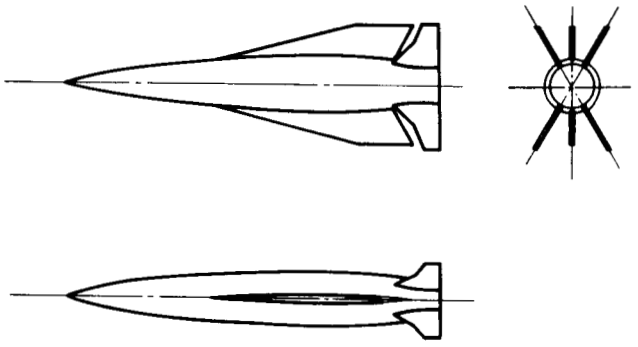

(a) MONOPLANAR MISSILE WITH CIRCULAR BODY

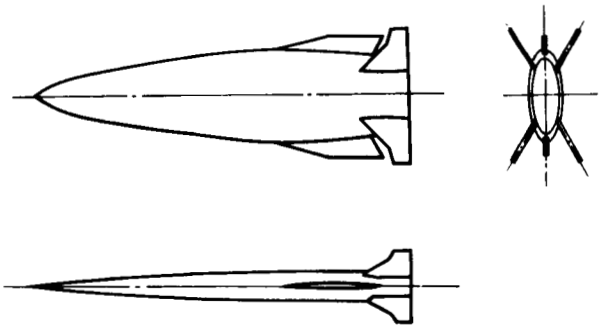

(b) MONOPLANAR MISSILE WITH ELLIPTICAL BODY

Figure 19.- Monoplanar missiles with circular or elliptical bodies.

NASA
National Aeronautics and Space Administration

Report Documentation Page

1. Report No.	2. Government Accession No.	3. Recipient's Catalog No.
NASA TM-100063		

4. Title and Subtitle
The Present Status and the Future of Missile Aerodynamics

5. Report Date
January 1988

6. Performing Organization Code

7. Author(s)
Jack N. Nielsen

8. Performing Organization Report No.
A-87289

10. Work Unit No.

9. Performing Organization Name and Address
Ames Research Center
Moffett Field, CA 94035

11. Contract or Grant No.

13. Type of Report and Period Covered
Technical Memorandum

12. Sponsoring Agency Name and Address
National Aeronautics and Space Administration
Washington, DC 20546-0001

14. Sponsoring Agency Code

15. Supplementary Notes
Point of Contact: Jack N. Nielsen, Ames Research Center, MS 200-1A
Moffett Field, CA 94035 (415) 694-5500 or FTS 464-5500

16. Abstract
This paper reviews some recent developments in the state of the art in missile aerodynamics. Among the subjects covered are (1) Tri-service/NASA data base, (2) wing-body interference, (3) nonlinear controls, (4) hypersonic transition, (5) vortex interference, (6) airbreathers, supersonic inlets, (7) store separation problems, (8) correlation of missile data, (9) CFD codes for complete configurations, (10) engineering prediction methods, and (11) future configurations. Throughout the paper, suggestions are made for future research and development to advance the state of the art of missile aerodynamics.

17. Key Words (Suggested by Author(s))	18. Distribution Statement
Tactical missiles Stability and control Review of present and future missiles	Unclassified-Unlimited Subject Category - 02

19. Security Classif. (of this report)	20. Security Classif. (of this page)	21. No. of pages	22. Price
Unclassified	Unclassified	35	A03